

# Torque Ripple Minimization and Performance Investigation of an In-Wheel Permanent Magnet Motor

Ali Mansouri  
CES Laboratory  
Engineering School of Sfax  
Tunisia  
Ali.Mansouri@isetgf.rnu.tn

Trabelsi Hafedh  
CES Laboratory  
Engineering School of Sfax  
Tunisia  
hafedh.trabelsi@enis.rnu.tn

**Abstract**—Recently, electric vehicle motoring has become a topic of interest, due to the several problems caused by thermal engines such as pollution and high oil prices. Thus, electric motors are increasingly applied in vehicle' applications and relevant research about these motors and their applications has been performed. Of particular interest are the improvements regarding torque production capability, the minimization of torque ripple and iron losses. The present work deals with the optimum design and the performance investigation of an outer rotor permanent magnet motor for in-wheel electric vehicle application. At first, and in order to find the optimum motor design, a new based particle-swarm multi-objective optimization procedure is applied. Three objective functions are used: efficiency maximization, weight and ripple torque minimization. Secondly, the effects of the permanent magnets segmentation, the stator slots opening, and the separation of adjacent magnets by air are outlined. The aim of the paper is the design of a topology with smooth output torque, low ripple torque, low iron losses and mechanical robustness.

**Keywords**-permanent magnet motor; optimization; performance; magnets design; ripple torque

## I. INTRODUCTION

In recent years, permanent magnet machines (PMM) have become widely used in different industrial applications [1-4]. This is essentially due to their miscellaneous advantages: higher efficiency, compact structure, smaller size, lower weight and flexibility of control. Depending on the permanent magnets magnetization, three types of machines can be distinguished: the radial flux machine [5], the axial flux [6] and the transverse flux ones [7]. Based on the arrangement of the rotor, two configurations may be encountered: the machine with an internal rotor and the machine with external rotor. In our work, the investigated topology is a surface mounted permanent magnet motor with an outer rotor and concentrated windings which is applied for in-wheel electric vehicle. The choice of the outer rotor configuration can be justified by the fact that this machine has a large air gap diameter, allowing a large number of poles. Also, because of the fact that it is most suitable for direct integration in the vehicle wheel, making more compact

the overall system. Further, during the rotor rotation, the centrifugal forces exert a pressure on the permanent magnets, making their detachment more difficult.

The magnetic circuit of a permanent magnet motor is very complex, nonlinear and characterized by a high number of parameters making its design a difficult task. In this case, an artificial intelligence technique is used. In the present work, a new based particle swarm optimization (PSO) method is applied [8]. An optimized design is selected and studied by means of finite element analysis (FEA) tool. Then FEA results are compared with those obtained by the optimization procedure. In order to reach the best machine performance, the effects of different parameters such as magnets segmentation, slot opening and adjacent magnets separation by air are outlined.

## II. STUDIED TOPOLOGY

In the present work, the investigated machine topology is a 26 kW, 3-phase, 18-poles, 27 stator slots and concentrated windings synchronous surface-mounted permanent magnet motor with an outer rotor. The stator is made up of laminated iron core and a three phase stator windings. The rotor consists of thin permanent magnets mounted in an iron core. The magnets, alternatively magnetized in a radial direction, produce a magnetic field across the air gap. Then, this magnetic field reacts with currents in windings placed in stator slots to produce the output torque. A general layout of the studied machine is illustrated in Figure 1.

The materials used to define the physical properties of the different regions analyzed by the finite element analysis are as follows:

- A linear model of rare earth Neodymium-Iron-Boron (NdFeB) permanent magnet material characterized by constants values: the relative permeability  $\mu_r$ , the coercive force  $H_c$  and residual flux density  $B_r$ .
- For iron parts (stator and rotor core), a non-linear laminated iron model (M800-65A).

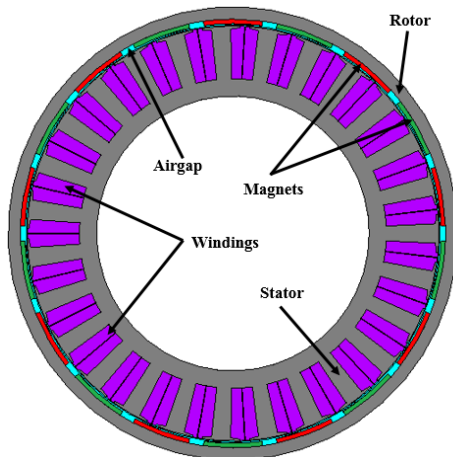


Fig. 1. Machine layout.

### III. ARTIFICIAL INTELLIGENT TECHNIQUE AND OPTIMIZATION PROCEDURE

Several electric machines optimization techniques have been proposed. From these techniques, we can distinguish, essentially, those based on the Genetic and the particle swarm optimization (PSO) algorithms which are the two most popular methods in electrical machine design and optimization [9-12]. In this work, we have used an optimization method based on the second algorithm: the Speed-constrained Multi-objective PSO (SMPSO) algorithm [8].

In cases where the speed is too high, the proposed method enables the generation of new efficient particle locations. Other characteristics of the SMPSO algorithm are: the use of an external archive to save the non-dominated solutions found during the search, and the use of polynomial mutation as a turbulence factor [8]. Compared to other multi-objective optimization algorithms, the SMPSO algorithm performs better in terms of speed convergence to the Pareto front, and of quality of the approximations of the found Pareto front.

In order to find the optimum geometric parameters of the investigated permanent magnet machine, an optimization procedure, based on the PSO algorithm, was performed. These design parameters are: the airgap length  $\delta$ , the rotor inner diameter  $D_{rint}$ , the magnets height  $h_m$ , the slot wedge height  $h_{sw}$ , the stator teeth width  $b_{ts}$ , the stator slot height  $h_s$ , the opening slot factor  $k_{open}$ , the active machine length  $l$ , the pole angle  $\alpha$ , and the stator inner diameter  $D_{sint}$ . These parameters are shown in Figure 2. In this paper, and in order to implement the optimization procedure, an analytical model, dealing with the magnetic and electric machine features is required. Such model has been developed in previous works [13-14], and it is summarized as follows:

- Maximum value of the airgap flux density created by the permanent magnets:

$$B_m = \frac{h_m}{h_m + \mu_r \delta_e} B_r \quad (1)$$

where  $\delta_e$  is the effective airgap length and  $kc$  is the Carter coefficient.

- Peak air gap flux density:

$$B_g = \frac{4}{p} B_m \sin\left(\frac{\alpha_{pm} p}{2}\right) \quad (2)$$

where  $\alpha_{pm}$  is the relative magnet width.

- Stator tooth flux density:

$$B_{st} = \frac{l' \tau_s B_m}{k_{fer} l b_{ts}} \quad (3)$$

where  $k_{fer}$ ,  $\tau_s$  and  $l'$  are the stacking factor of the stator iron laminations which is taken equal to 0.95, the slot pitch and the iron core length.

- Stator and rotor yokes flux densities:

$$B_{sy} = \frac{\tau_p B_g}{2 h_{sy} k_{fer}} \quad (4)$$

$$B_{ry} = \frac{\tau_m B_m}{2 h_{ry} k_{fer}} \quad (5)$$

where  $\tau_m$ ,  $h_{sy}$ ,  $\tau_p$  and  $h_{ry}$  are respectively the magnet pitch, the stator yoke height, the pole pitch and the rotor yoke height.

- Fundamental of the phase electromotive force:

$$\hat{E}_{a,1} = \pi \sqrt{2} f N_c B_g k_{w1} \frac{D_{sext} l'}{p} \quad (6)$$

where  $f$ ,  $N_c$ ,  $D_{sext}$ ,  $p$  and  $k_{w1}$  are respectively the electrical frequency, the number of turns of windings of a phase, the stator outer diameter, the pole pairs number and the fill factor.

- Electromagnetic torque:

$$T_{rms} = \frac{\pi}{4} B_g \hat{I}_s D_{sext}^2 l' \sin \beta \quad (7)$$

where  $\hat{I}_s$ ,  $\beta$  and  $\hat{S}_I$  are respectively the amplitude of the fundamental current of a phase, the electrical angle between the current and the magnet flux vector and the amplitude of the fundamental component of electric loading.

- Copper losses

$$P_{cu} = 3 R_{ph} I_{ph}^2 \quad (8)$$

$I_{ph}$  is the phase current and  $R_{ph}$  is the phase resistance.

• Iron losses:

$$P_{st} = \left( k_h f B_{st}^\beta + \pi^2 \frac{\sigma d^2}{6} B_{st}^2 f^2 + 8.67 k_c f^{1.5} B_{st}^{1.5} \right) V_{st} \quad (9)$$

$$P_{sy} = \left( k_h f B_{sy}^\beta + \pi^2 \frac{\sigma d^2}{6} B_{sy}^2 f^2 + 8.67 k_c f^{1.5} B_{sy}^{1.5} \right) V_{sy} \quad (10)$$

$$P_{ry} = \left( k_h f B_{ry}^\beta + \pi^2 \frac{\sigma d^2}{6} B_{ry}^2 f^2 + 8.67 k_c f^{1.5} B_{ry}^{1.5} \right) V_{ry} \quad (11)$$

where  $P_{st}$ ,  $P_{sy}$ ,  $P_{ry}$ ,  $k_h$ ,  $\beta$ ,  $\sigma$ ,  $d$ ,  $k_c$ ,  $V_{st}$ ,  $V_{sy}$  and  $V_{ry}$ , the stator tooth losses, the stator yoke losses, the rotor yoke losses, the hysteresis coefficient, the Steinmetz constant, the iron lamination conductivity, the lamination thickness, the excess losses coefficient, the stator teeth, stator yoke and rotor yoke volumes.

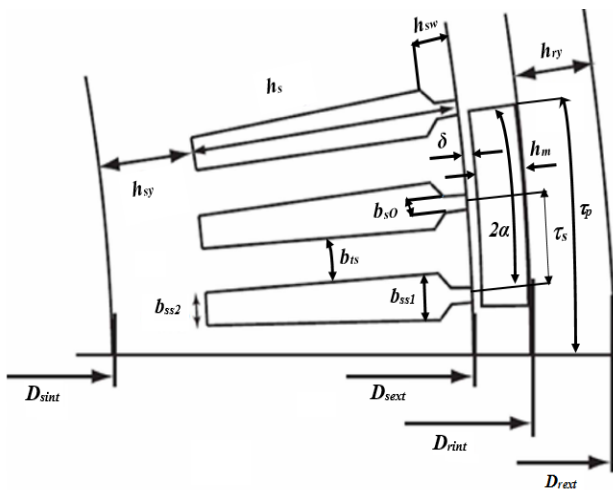


Fig. 2. Machine layout Basic machine geometric dimensions.

In the present work, three objective functions were carried out; the efficiency maximization, the machine weight and ripple torque minimization:

$$\text{objective\_function1} = \text{minimum}(1 - \eta) \quad (12)$$

where  $\eta$  is machine efficiency defined by:

$$\eta = \frac{P_{out}}{P_{out} + P_{cu} + P_{st} + P_{sy} + P_{ry}} \quad (13)$$

$P_{out}$ ,  $P_{cu}$ ,  $P_{st}$ ,  $P_{sy}$ ,  $P_{ry}$  are respectively the machine output power, the copper losses, the stator teeth losses, the stator yoke losses and the rotor yoke losses.

The second objective function is described by the following equation:

$$\text{objective\_function2} = \text{minimum}(\text{weight}) \quad (14)$$

where “weight” is the total machine weight.

The third objective function is the ripple torque minimization:

$$\text{objective\_function3} = \text{minimum}(T_{rip}) \quad (15)$$

where,  $T_{rip}$ , is the ripple torque which can be evaluated analytically from the harmonics in the back-EMF [15]:

$$T_{rip} = 2 \sqrt{\frac{(\hat{E}_7 - \hat{E}_5)^2 + (\hat{E}_{13} - \hat{E}_{11})^2 + (\hat{E}_{19} - \hat{E}_{17})^2 + (\hat{E}_{25} - \hat{E}_{23})^2}{\hat{E}_1}} \quad (16)$$

where  $\hat{E}_i$  is the amplitude of the  $i^{\text{th}}$  harmonic component of the back-EMF.

Afterwards, the optimization procedure was implemented and run many times. As first results of the optimization process, we are interested to the Pareto fronts, which are illustrated in Figures 3-5. From these fronts, the designer should select the points meeting the specific design requirements. All front values are feasible and the choice can be made by considering other features that the motor must have. Referring to these figures, we notice the tradeoff between the weight, the efficiency and the ripple torque. Thereafter increasing the efficiency, leads to machine weight and ripple torque increase. This is due to the fact that when the weight increases, the machine can be designed with lower magnetic and electric loading.

In order to verify the accuracy of the proposed optimization procedure, an optimized topology, whose parameters are given in Table I, was selected and analyzed by FEA. The obtained results, for the most relevant parameters, are provided in Table II.

TABLE I. OPTIMIZED TOPOLOGY PARAMETERS

Parameter	Value
$\delta$ (mm)	1.6
$D_{rint}$ (mm)	285.6
$h_m$ (mm)	3
$h_{sw}$ (mm)	2.1
$b_{is}$ (mm)	13
$K_{open}$	0.5
$h_s$ (mm)	35.2
$l$ (mm)	50
$\alpha$ (°)	16
$D_{sint}$ (mm)	183
Efficiency (%)	0.981
weight (kg)	31.44
CPU (s)	8.672
$T_{rip}$ (%)	37

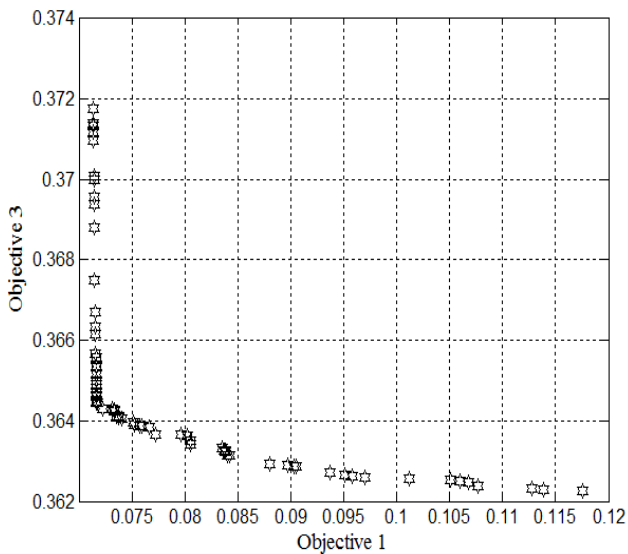


Fig. 3. Pareto front for objective functions 1-3

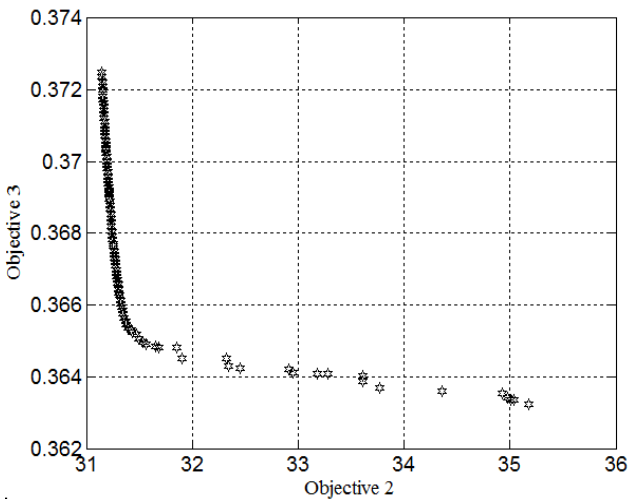


Fig. 4. Pareto front for objective functions 2-3

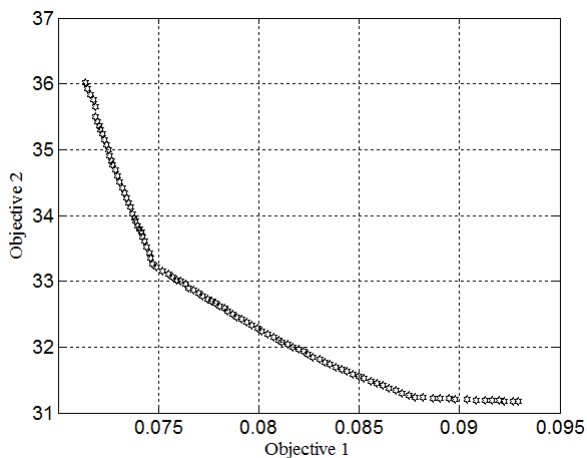


Fig. 5. Pareto front objective functions 1-2

TABLE II. COMPARISON BETWEEN FEA RESULTS AND OPTIMIZATION RESULTS

Parameter	Optimization	FEA
Magnet flux density $B_m$ (T)	0.7	0.72
Airgap flux density $B_g$ (T)	0.85	0.91
Stator yoke flux density $B_{sv}$ (T)	1.7	1.77
Stator teeth flux density $B_{st}$ (T)	2	1.85
Rotor yoke flux density $B_{rv}$ (T)	1.86	2.1
Torque ripple $T_{rip}$ (%)	37.5	42
Iron losses (kW)	1.057	1.064

IV. MACHINE PERFORMANCES AMELIORATION

A. Magnet segmentation effect

For the purpose of showing the magnet segmentation effect on the output torque and on the torque ripple, the magnets are divided into segments on the radial direction as illustrated in Figure 6. FEA Computation results of the machine output torque are illustrated in Figure 7 and Table III. According to these results, the maximum output torque and the lower ripple torque are provided in the 8 segments-magnets topology.

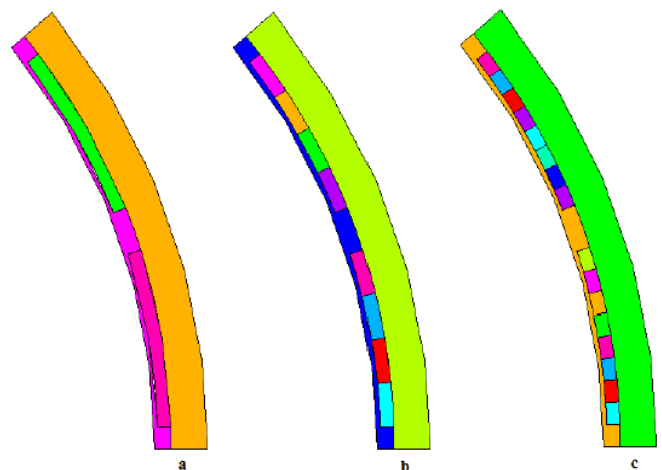


Fig. 6. Different rotor structures: a: 2 segments, b: 4 segments and c: 8 segments.

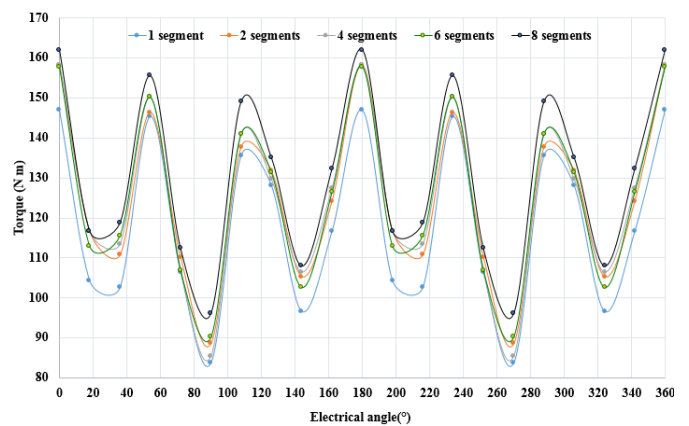


Fig. 7. Torque variation for different magnet segmentation numbers

TABLE III. TORQUE RIPPLE VERSUS NUMBER OF MAGNETS NUMBER

Number of magnets segments	Torque ripple (%)
1	43
2	44
3	47
4	46
5	43
6	42
7	44
8	40

B. Effect of air width between adjacent magnets

With the aim of improving the machine performances and reduce the torque ripple, adjacent magnet segments are separated by air as illustrated in Figure 8. In this case, the effect of the air width on the machine performance has to be investigated. FEA calculation dealing with this parameter are illustrated in Figures 9 and 10. Based on these figures, it is shown that the output torque increases with the air width until it reaches a maximum value corresponding to an air length equal to 0.45° and after that it decreases. This is due to the fact that on one hand the saturation in the rotor poles increases with the magnet width, and on the other hand, to the increase of the flux linkage between the stator and the rotor when the magnet width increases. Referring to Figure 7, we can note the decrease of the torque ripple as function of the air width to achieve a minimum value, corresponding to an air length of 0.55°, and then its increase with the same parameter.

C. Slot opening effect

Another influent parameter is the stator slot opening. This parameter influences directly the air gap magnetic field in two ways. It decreases the average flux density and it affects the flux density distribution through the air gap. These two effects are illustrated in Figure 11 for semi closed and fully opened slots.

V. CONCLUSION

This paper investigates the optimization and performance investigation of a surface mounted outer rotor and concentrated windings permanent magnet machine designed for in-wheel application. At first, an optimization procedure based on the improved PSO multi-Objective optimization algorithm was implemented. The goal of this optimization procedure is to find the optimum machine's geometric parameters providing the maximum efficiency and the minimum weight and ripple torque. Afterwards, an optimized topology is selected and analyzed by FEA. Simulation results illustrates that the results obtained by analytical optimization are in good agreement with those obtained by FEA. Magnet segmentation, air between adjacent magnet segments width and slot opening effects are investigated with FEA. Based on the obtained results, it is shown that a higher number of magnet segments leads to higher output torque. It is also shown that the output torque increases with the air between adjacent magnet segments width, until it reaches a maximum value corresponding to a magnet segments width of 0.45°. Subsequently, the slotting effect on the airgap flux density is investigated. In this case, it is illustrated that both magnetic flux density average and distribution are influenced by this parameter.

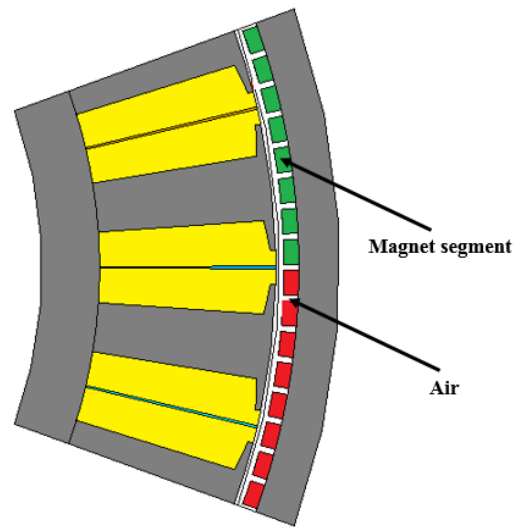


Fig. 8. Topology with air between adjacent magnets.

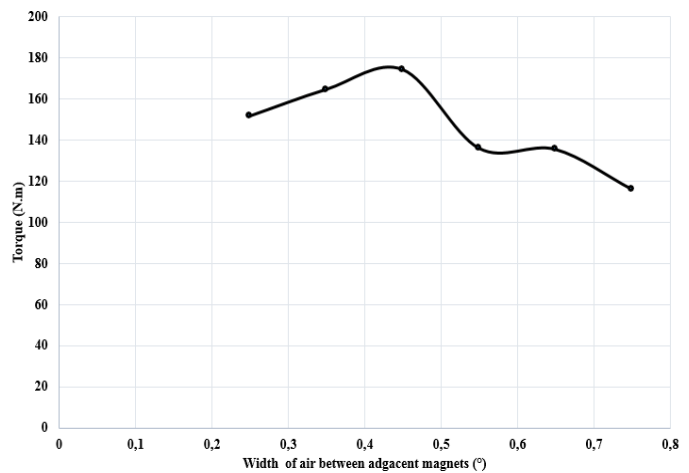


Fig. 9. Maximum output torque versus air between adjacent magnets width.

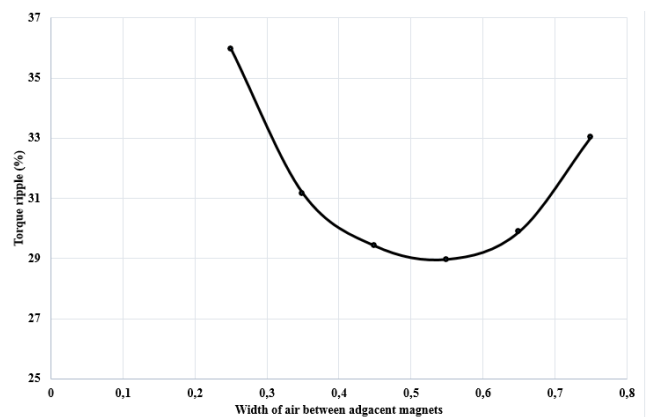


Fig. 10. Ripple torque versus air between adjacent magnets width.

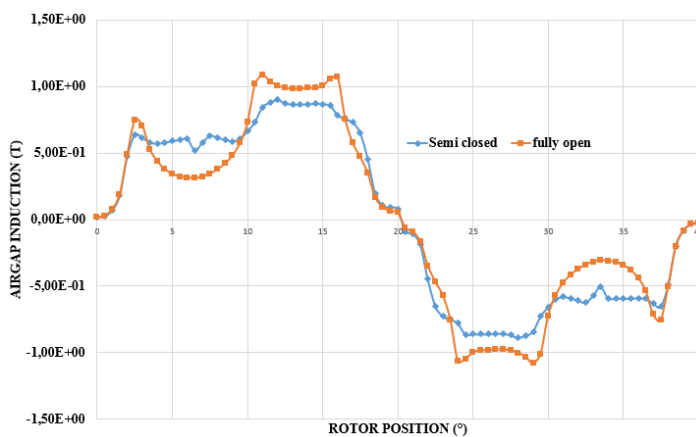


Fig. 11. Airgap flux density versus rotor position for semi closed and fully opened slots.

[14] A. Mansouri, N. Smairi, H. Trabelsi, "A new multi-objective optimization procedure based on particle swarm algorithm for optimum design of in-wheel permanent magnet motor", *Tur. J. Elec. Eng. Comp. Sci.* (submitted)

[15] S. Huang, M. Aydin, T. Lipo, "Comparison of (non-slotted and slotted) surface mounted PM motors and axial flux motors for submarine ship drives," in *Proc. of 3rd Naval Symposium on Electrical Machines, USA, Dec. 4-7, 2000*

#### REFERENCES

- [1] Z. Q. Zhu, D. Howe, "Electrical machines and drives for electric, hybrid and fuel cell vehicles", *Proc. in the IEEE*, Vol. 95, No. 4, pp. 746–765, 2007
- [2] J. Wang, K. Atallah, Z. Q. Zhu, D. Howe, "Modular 3-phase permanent magnet brushless machines for in-wheel applications", *IEEE T. Veh. Technol.*, Vol. 57, No. 5, pp. 2714-2720, 2008
- [3] Y. Chen, P. Pillay, A. Khan, "PM wind generator topologies", *IEEE T. Ind. Appl.*, Vol. 41, No. 6, pp. 619-1626, 2005
- [4] X. Sun, C. Ming, W. Hua, L. Xu, "Optimal design of double layer permanent magnet dual mechanical port machine for wind power application", *IEEE T. Magn.*, Vol. 45, No. 10, pp. 4613–4616, 2009
- [5] F. Libert, *Design, Optimization and Comparison of Permanent Magnet Motors for a Low-Speed Direct-Driven Mixer*, Ph.D. Thesis, Royal Institute of Technology, Sweden, 2004
- [6] L. Brooke, *Protean electric tackles the unsprung-mass 'myth' of in-wheel motors*, 2011 SAE World Congress, USA, 2011
- [7] H. Weh, "Ten years of research in the field of high force density-transverse flux machines", In *Proc. speedam'96*, Capri, 1996
- [8] A. J. Nebro, J. J. Durillo, J. Garcia-Nieto, C. A. Coello Coello, F. Luna, E. Alba, "SMPPO: A New PSO-based Metaheuristic for Multi-objective Optimization", *IEEE 2009 Symposium on Computational Intelligence in Multi-criteria Decision-Making*, Nashville, TN, USA, 30 March-02 April 2009
- [9] R. Ilka, A. R. Tilaki, H. A. Alamdari, R. Baghipour, "Design Optimization of Permanent Magnet-Brushless DC Motor using Elitist Genetic Algorithm with Minimum loss and Maximum Power Density", *Int. J. Mecha. Electr. Comput. Technol.*, Vol. 4, No. 10, pp. 1169-1185 2014
- [10] Y. Ahn, J. Park, C. G. Lee, J. W. Kim, S. Y. Jung, "Novel Memetic Algorithm implemented With GA (Genetic Algorithm) and MADS (Mesh Adaptive Direct Search) for Optimal Design of Electromagnetic System", *IEEE T. Magn.*, Vol. 46, No. 6, pp. 1982–1985, 2010
- [11] V. P. Sakthivel, R. Bhuvaneswari, S. Subramanian, "Multi-objective parameter estimation of induction motor using particle swarm optimization", *Eng. Appl. Artif. Intel.*, Vol. 23, No. 3, pp. 302–312, 2010
- [12] M. Ashabani, Y. A. R. I. Mohamed, "Multi-objective Shape Optimization of Segmented Pole Permanent-Magnet Synchronous Machines with Improved Torque Characteristics", *IEEE T. Magn.*, Vol. 47, No. 4, pp. 795-804, 2011
- [13] A. Mansouri, N. Smairi, H. Trabelsi, "Multi-objective Optimization of an In-Wheel Electric Vehicle Motor", *Int. J. App. Elect. Mech.*, Vol. 50, No. 3, pp. 449-465, 2016